J. Fluid Mech. (2016), *vol.* 808, *pp.* 562–575.
doi:10.1017/jfm.2016.650

Energy dissipation rate limits for flow through rough channels and tidal flow across topography

R. R. Kerswell†

School of Mathematics, Bristol University, Bristol BS8 1TW, UK

(Received 3 August 2016; revised 28 September 2016; accepted 3 October 2016;
first published online 4 November 2016)

An upper bound on the energy dissipation rate per unit mass, ε, for pressure-driven flow through a channel with rough walls is derived for the first time. For large Reynolds numbers, Re, the bound – $\varepsilon \leqslant cU^3/h$ where U is the mean flow through the channel, h the channel height and c a numerical prefactor – is independent of Re (i.e. the viscosity) as in the smooth channel case but the numerical prefactor c, which is only a function of the surface heights and surface gradients (i.e. not higher derivatives), is increased. Crucially, this new bound captures the correct scaling law of what is observed in rough pipes and demonstrates that while a smooth pipe is a singular limit of the Navier–Stokes equations (data suggest $\varepsilon \sim 1/(\log Re)^2 U^3/h$ as $Re \to \infty$), it is a regular limit for current bounding techniques. As an application, the bound is extended to oscillatory flow to estimate the energy dissipation rate for tidal flow across bottom topography in the oceans.

Key words: Navier–Stokes equations, shear layer turbulence, variational methods

1. Introduction

In every turbulent flow, there is some key quantity of interest which is either enhanced or suppressed compared to its laminar value and it is of fundamental interest to understand this effect as a function of the parameters of the problem. Well-known examples include the mass flux along a channel driven by an applied pressure gradient, the heat flux across a differentially heated fluid layer or the wall shear stress exerted by a fluid sheared between two parallel plates. One approach is to derive strict inequality information on these key global flow quantities as a function of the system parameters in the hope that this captures the correct scaling relationship. This 'bounding' approach is attractive because it seeks to extract just enough of the physics from the governing equations to make the correct prediction while eschewing other secondary flow details which arise from directly solving the governing equations and just may not be attainable in the asymptotic regime of interest (e.g. vanishing viscosity). The downside of the bounding approach is that the bound derived can be too conservative. Well-known examples are the energy dissipation rate ε in a smooth pipe where the best (lowest) bound known predicts that ε approaches a finite constant (in units of U^3/h) as the Reynolds number Re becomes large – the so-called Kolmogorov scaling (Frisch 1995) – whereas data suggest a $\sim 1/(\log Re)^2$ drop off,

† Email address for correspondence: R.R.Kerswell@bristol.ac.uk

and the scaling of the Nusselt number Nu (normalised heat flux) in Boussinesq convection with Rayleigh number Ra: the bound has $Nu \lesssim Ra^{\alpha}$ with $\alpha = 1/2$ for $Ra \to \infty$ whereas current data suggest $\alpha \approx 0.31$ (e.g. see the discussion in Waleffe, Boonkasame & Smith (2015)) with probable dependence on the Prandtl number too (Grossmann & Lohse 2000).

The bounding approach owes its roots to a suggestion by Malkus (1954) that turbulent flows want to maximise their transport and was first applied in convection by Howard (1963) and in shear flows by Busse (1969, 1970) (see Howard (1972) and Busse (1978) for early reviews). The original approach was based on using certain simple projections of the governing equations as constraints in an optimisation problem. After initial successes, it quickly became hard to pose more constrained yet still tractable problems and the field languished in the late 70s and 80s. In the early 90s, a new 'background' method introduced by Doering & Constantin (1992, 1994, 1996), Constantin & Doering (1995) revitalised the field by providing an alternative way to systematically derive rigorous bounding results (Marchioro 1994; Kerswell 1996, 2002; Nicodemus, Grossmann & Holthaus 1997; Wang 1997; Hoffmann & Vitanov 1999; Doering & Constantin 2001; Doering & Foias 2002; Otero *et al.* 2002; Plasting & Kerswell 2003, 2005; Plasting & Ierley 2005; Wittenberg 2010; Whitehead & Doering 2011; Wen *et al.* 2013; Whitehead & Wittenberg 2014). The key idea (traceable back to Hopf) is to decompose the flow variables into a steady incompressible 'background' field which carries the inhomogeneities of the problem and a fluctuating incompressible part which is unforced and hence of arbitrary amplitude. The method then proceeds by designing the background field (typically with a boundary layer of thickness δ) so that the influence of the unknown fluctuating field on the key functional of interest can be bounded (by taking δ small enough). While very successful (e.g. see Wang (1997) for a proof of an upper bound on ε for a general domain where the boundary moves tangentially to itself everywhere), the method does have its limitations, most notably illustrated by the problem of pressure-driven flow across a rough wall (see also Nobili & Otto (2016) for work in the convection problem). In flow driven across a rough wall, the background flow must bring an $O(1)$ (relative to $\delta \to 0$) normal component of the exterior flow to zero at the rough wall surface over a boundary layer distance of $O(\delta)$. Incompressibility then forces the background flow to have an $O(1/\delta)$ component locally tangent to the rough wall and control of the unknown fluctuating part is lost (technically the required spectral constraint cannot be satisfied). Incompressibility of the background field is the key obstacle here: relaxing the constraint on the background field causes problems elsewhere (the fluid pressure cannot be eliminated from the analysis) or when it is not relevant – in the case of convection where only a background temperature field is needed – there is no problem (Goluskin & Doering 2016).

In the last 5 years, a second new bounding method has been developed by Otto & Seis (2011), Seis (2015) – hereafter referred to as the 'boundary layer' method – which potentially offers a new line of attack on the roughness problem. In this paper we discuss how this method can indeed be extended to deliver a first rigorous upper bound on the energy dissipation rate for pressure-driven flow through a rough channel. Interestingly, the same scaling law emerges for the bound on ε in terms of the applied pressure gradient as for the smooth channel situation (albeit with an enlarged numerical prefactor dependent on the exact form of the roughness). This is exactly what has also been found very recently for rough wall convection (using the background technique) in Goluskin & Doering (2016). Assuming the bound carries over to rough pipe flow, this then matches the observed scaling law for turbulent data

(Moody 1944). There are two immediate implications: (i) a smooth wall is a singular limit of rough wall flows at high Re flows yet a regular limit for current upper bounding techniques; and (ii) current upper bounding techniques are actually better at capturing scaling laws than has been immediately apparent by focussing on the singular case of smooth wall problems (see Goluskin & Doering (2016) for references which suggest that their rough wall bound may be consistent with convection data). To illustrate how the new energy dissipation rate bound can be utilized, we extend the result to oscillatory free-surface flow over one rough boundary which is a simple model of tidal flow over topography. Understanding how topography such as isolated ridges enhance dissipation and especially mixing processes is an important yet poorly understood ingredient for ocean circulation modelling (e.g. see Melet, Legg & Hallberg (2016) and references therein).

2. Three-dimensional rough channel flow

Imagine a channel of average height h, periodic extent hL_x in the (streamwise) direction of an applied pressure gradient and periodic spanwise extent hL_y. If ν is the kinematic viscosity, then introduce ν/h as the unit of speed, h as the unit of length and h^2/ν as the unit of time. The governing Navier–Stokes equations become

$$\frac{\partial \boldsymbol{u}}{\partial t} + \boldsymbol{u}\cdot\boldsymbol{\nabla}\boldsymbol{u} + \boldsymbol{\nabla} p - \nabla^2\boldsymbol{u} = Gr\hat{\boldsymbol{x}}, \tag{2.1}$$

$$\boldsymbol{\nabla}\cdot\boldsymbol{u} = 0, \tag{2.2}$$

where $Gr := h^3\mathcal{G}/\nu^2$, the Grashof number, is the non-dimensionalised applied pressure gradient $\mathcal{G}$ driving the flow. For convenience, we refer to the cross-channel z-direction as the 'vertical' direction and the x and y directions as 'horizontal' and imagine rough channel boundaries at $z = f(x, y)$ (the lower boundary) and $z = g(x, y)$ (the upper boundary). The roughness functions f and g will be assumed at least C^3 (3 times differentiable), periodic over $\mathcal{A} := [0, L_x] \times [0, L_y]$ such that

$$\iint_{\mathcal{A}} f \,\mathrm{d}x\,\mathrm{d}y = 0 \quad \text{and} \quad \frac{1}{A}\iint_{\mathcal{A}} g \,\mathrm{d}x\,\mathrm{d}y = 1 \tag{2.3a,b}$$

(to preserve the average channel height as 1 in non-dimensional units and non-dimensional volume as $A := L_xL_y$) and to be such that the channel is never blocked at any point (i.e. $f < g$ for any $(x, y) \in \mathcal{A}$). In the following we work with a one-dimensional (1-D) family of interior surfaces

$$\mathcal{S}(\lambda) := \{(x, y, z) | z = F(x, y, \lambda) := (1-\lambda)f(x, y) + \lambda g(x, y) \text{ for } (x, y) \in \mathcal{A}\} \tag{2.4}$$

with $\lambda \in [0, 1]$ which smoothly interpolate between the two rough boundaries: $\lambda = 0$ giving the lower boundary and $\lambda = 1$ the upper boundary: see figure 1. Let $\mathcal{C}(\lambda, y^*)$ be the line formed from the intersection of $\mathcal{S}(\lambda)$ with the $y = y^*$ plane. Let $\mathcal{V}(\lambda)$ be the volume enclosed by $\mathcal{S}(\lambda)$, $\mathcal{S}(0)$ (the lower boundary) and the planes $x = 0$, $x = L_x$, $y = 0$ and $y = L_y$, and let $\partial\mathcal{V}(\lambda)$ be the boundary of $\mathcal{V}(\lambda)$. The flow conditions at the edges of each surface are periodic so that the flow is invariant under the transformations $x \to x + L_x$ and $y \to y + L_y$. A long-time average is defined as

$$\big\langle (\cdot) \big\rangle := \lim_{T\to\infty} \frac{1}{T}\int_0^T (\cdot)\,\mathrm{d}t. \tag{2.5}$$

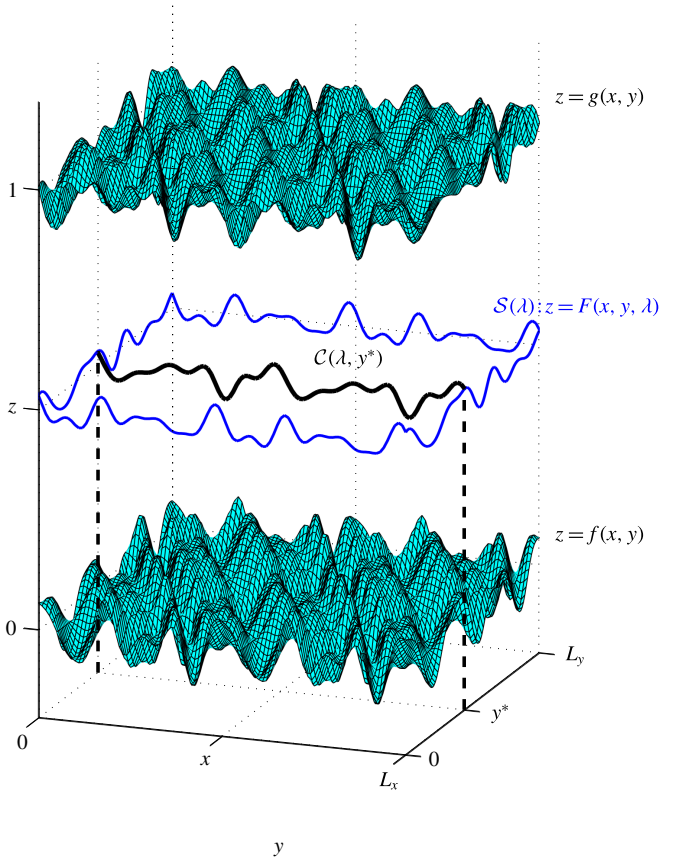

FIGURE 1. (Colour online) The flow geometry. The top boundary is given by $z = g(x, y)$ and the bottom by $z = f(x, y)$. The intermediate surface shown in outline is parametrised by λ and defined by $z = F(x, y, \lambda) := (1 - \lambda)f(x, y) + \lambda g(x, y)$.

We start the 'boundary layer' bounding analysis (Otto & Seis 2011; Seis 2015) by taking the line integral of (2.1) along $\mathcal{C}(\lambda, y)$ (in the direction of increasing x) followed by an integration over y,

$$\int_0^{L_y} \int_{\mathcal{C}(\lambda,y)} \hat{\boldsymbol{s}} \cdot \left[\frac{\partial \boldsymbol{u}}{\partial t} + \boldsymbol{u} \cdot \boldsymbol{\nabla} \boldsymbol{u} + \boldsymbol{\nabla} p - \nabla^2 \boldsymbol{u} \right] \mathrm{d}s \, \mathrm{d}y = Gr \int_0^{L_y} \int_{\mathcal{C}(\lambda,y)} \hat{\boldsymbol{s}} \cdot \hat{\boldsymbol{x}} \, \mathrm{d}s \, \mathrm{d}y, \tag{2.6}$$

where s is the arc-length along $\mathcal{C}(\lambda, y)$ and $\hat{\boldsymbol{s}} := (\hat{\boldsymbol{x}} + F_x \hat{\boldsymbol{z}})/\sqrt{1 + F_x^2}$ is the unit tangent vector (subscripts indicate partial derivatives so that $F_x = \partial F/\partial x$ with y and λ held fixed). Crucially, this procedure kills the pressure term as

$$\int_{\mathcal{C}(\lambda,y)} \hat{\boldsymbol{s}} \cdot \boldsymbol{\nabla} p \, \mathrm{d}s = p(L_x, y, F(L_x, y, \lambda), t) - p(0, y, F(0, y, \lambda), t) = 0 \tag{2.7}$$

by periodicity in x. With this, and converting the line integral to an integration over x, we get

$$A\, Gr = \frac{\partial}{\partial t} \iint_{\mathcal{A}} (\hat{\boldsymbol{x}} + F_x \hat{\boldsymbol{z}}) \cdot \boldsymbol{u} \, \mathrm{d}x \, \mathrm{d}y + \iint_{\mathcal{A}} (\hat{\boldsymbol{x}} + F_x \hat{\boldsymbol{z}}) \cdot [\boldsymbol{u} \cdot \boldsymbol{\nabla} \boldsymbol{u} - \nabla^2 \boldsymbol{u}] \, \mathrm{d}x \, \mathrm{d}y. \tag{2.8}$$

The first term on the right-hand side can be dropped after long-time averages, assuming that the kinetic energy remains bounded in time, to leave

$$Gr = \left\langle \frac{1}{A} \iint_{\mathcal{A}} (\hat{\boldsymbol{x}} + F_x \hat{\boldsymbol{z}}) \cdot [\boldsymbol{u} \cdot \boldsymbol{\nabla} \boldsymbol{u} - \nabla^2 \boldsymbol{u}] \, \mathrm{d}x \, \mathrm{d}y \right\rangle , \tag{2.9}$$

which is an identity for any $\lambda \in [0, 1]$. We now generate volume integrals from this expression which can be related to the long-time-averaged energy dissipation rate per unit mass (in units of ν^3/h^4)

$$\varepsilon := \left\langle \frac{1}{A} \iiint |\boldsymbol{\nabla} \boldsymbol{u}|^2 \, \mathrm{d}V \right\rangle := \left\langle \frac{1}{A} \int_0^{L_x} \int_0^{L_y} \int_{z=f(x,y)}^{z=g(x,y)} |\boldsymbol{\nabla} \boldsymbol{u}|^2 \, \mathrm{d}z \, \mathrm{d}y \, \mathrm{d}x \right\rangle . \tag{2.10}$$

To do this, (2.9) is integrated over $\lambda \in [0, \Lambda]$ to give

$$\Lambda Gr = \left\langle \frac{1}{A} \int_0^{\Lambda} \iint_{\mathcal{A}} (\hat{\boldsymbol{x}} + F_x \hat{\boldsymbol{z}}) \cdot [\boldsymbol{u} \cdot \boldsymbol{\nabla} \boldsymbol{u} - \nabla^2 \boldsymbol{u}] \, \mathrm{d}x \, \mathrm{d}y \, \mathrm{d}\lambda \right\rangle . \tag{2.11}$$

This can be converted into a volume integral by converting the integral over λ to one over z with the addition of a (Jacobian) scaling factor $\partial z/\partial \lambda|_{x,y} = F_\lambda(x, y, \lambda)$:

$$\Lambda Gr = \left\langle \frac{1}{A} \iiint_{\mathcal{V}(\Lambda)} \boldsymbol{a} \cdot [\boldsymbol{u} \cdot \boldsymbol{\nabla} \boldsymbol{u} - \nabla^2 \boldsymbol{u}] \, \mathrm{d}x \, \mathrm{d}y \, \mathrm{d}z \right\rangle \quad \forall \Lambda \in [0, 1], \tag{2.12}$$

where

$$\boldsymbol{a} := \frac{\hat{\boldsymbol{x}} + F_x \hat{\boldsymbol{z}}}{F_\lambda} = \frac{\hat{\boldsymbol{x}} + [f_x + (z - f)[\ln(g - f)]_x]\hat{\boldsymbol{z}}}{(g - f)} \tag{2.13}$$

eliminating λ in favour of z (recall $g = g(x, y)$ and $f = f(x, y)$). The key now is to lift spatial derivatives off $\boldsymbol{u}$ and onto $\boldsymbol{a}$ by judicious use of the divergence theorem. This leads to

$$\begin{aligned} \Lambda Gr \; = \; & \frac{1}{A} \left\langle \oint_{\partial \mathcal{V}(\Lambda)} (\boldsymbol{a} \cdot \boldsymbol{u}) \boldsymbol{u} \cdot \hat{\boldsymbol{n}} + \boldsymbol{u} \cdot (\hat{\boldsymbol{n}} \cdot \boldsymbol{\nabla}) \boldsymbol{a} - \boldsymbol{a} \cdot (\hat{\boldsymbol{n}} \cdot \boldsymbol{\nabla}) \boldsymbol{u} \, \mathrm{d}S \right. \\ & \left. - \iiint_{\mathcal{V}(\Lambda)} \boldsymbol{u} \cdot (\boldsymbol{u} \cdot \boldsymbol{\nabla}) \boldsymbol{a} + \boldsymbol{u} \cdot \nabla^2 \boldsymbol{a} \, \mathrm{d}V \right\rangle \quad \forall \Lambda \in [0, 1] \end{aligned} \tag{2.14}$$

(note the last term requires the roughness functions f and g to be at least C^3). Due to periodicity over $(x, y) \in [0, L_x] \times [0, L_y]$, the only parts of $\partial \mathcal{V}(\Lambda)$ which need to be considered are the lower boundary $\mathcal{S}(0)$ where $\boldsymbol{u} = \boldsymbol{0}$ and the interior surface $\mathcal{S}(\Lambda)$. Hence, in fact

$$\begin{aligned} \Lambda Gr \; = \; & \frac{1}{A} \left\langle \int_{\mathcal{S}(\Lambda)} (\boldsymbol{a} \cdot \boldsymbol{u}) \boldsymbol{u} \cdot \hat{\boldsymbol{n}} + \boldsymbol{u} \cdot (\hat{\boldsymbol{n}} \cdot \boldsymbol{\nabla}) \boldsymbol{a} - \boldsymbol{a} \cdot (\hat{\boldsymbol{n}} \cdot \boldsymbol{\nabla}) \boldsymbol{u} \, \mathrm{d}S \right. \\ & - \int_{\mathcal{S}(0)} \boldsymbol{a} \cdot (\hat{\boldsymbol{n}} \cdot \boldsymbol{\nabla}) \boldsymbol{u} \, \mathrm{d}S \\ & \left. - \iiint_{\mathcal{V}(\Lambda)} \boldsymbol{u} \cdot (\boldsymbol{u} \cdot \boldsymbol{\nabla}) \boldsymbol{a} + \boldsymbol{u} \cdot \nabla^2 \boldsymbol{a} \, \mathrm{d}V \right\rangle \quad \forall \Lambda \in [0, 1]. \end{aligned} \tag{2.15}$$

Now the strategy is to separately average (2.15) over $\Lambda \in [0, \ell]$ and over $\Lambda \in [1-\ell, 1]$ and then compute the difference in order to eliminate the Λ-independent $\mathcal{S}(0)$ boundary term. Subtracting $1/\ell \int_0^\ell$ (2.15) $\mathrm{d}\Lambda$ from $1/\ell \int_{1-\ell}^1$ (2.15) $\mathrm{d}\Lambda$ gives

$$\begin{aligned}(1-\ell)Gr \;=\; \frac{1}{A}\Bigg\langle \frac{1}{\ell}\int_{1-\ell}^{1}\int_{\mathcal{S}(\Lambda)} (\boldsymbol{a}\cdot\boldsymbol{u})\boldsymbol{u}\cdot\hat{\boldsymbol{n}} + \boldsymbol{u}\cdot(\hat{\boldsymbol{n}}\cdot\boldsymbol{\nabla})\boldsymbol{a} - \boldsymbol{a}\cdot(\hat{\boldsymbol{n}}\cdot\boldsymbol{\nabla})\boldsymbol{u}\,\mathrm{d}S\,\mathrm{d}\Lambda \\ - \frac{1}{\ell}\int_{0}^{\ell}\int_{\mathcal{S}(\Lambda)} (\boldsymbol{a}\cdot\boldsymbol{u})\boldsymbol{u}\cdot\hat{\boldsymbol{n}} + \boldsymbol{u}\cdot(\hat{\boldsymbol{n}}\cdot\boldsymbol{\nabla})\boldsymbol{a} - \boldsymbol{a}\cdot(\hat{\boldsymbol{n}}\cdot\boldsymbol{\nabla})\boldsymbol{u}\,\mathrm{d}S\,\mathrm{d}\Lambda \\ - \frac{1}{\ell}\int_{1-\ell}^{1}\iiint_{\mathcal{V}(\Lambda)} \boldsymbol{u}\cdot(\boldsymbol{u}\cdot\boldsymbol{\nabla})\boldsymbol{a} + \boldsymbol{u}\cdot\boldsymbol{\nabla}^2\boldsymbol{a}\,\mathrm{d}V\,\mathrm{d}\Lambda \\ + \frac{1}{\ell}\int_{0}^{\ell}\iiint_{\mathcal{V}(\Lambda)} \boldsymbol{u}\cdot(\boldsymbol{u}\cdot\boldsymbol{\nabla})\boldsymbol{a} + \boldsymbol{u}\cdot\boldsymbol{\nabla}^2\boldsymbol{a}\,\mathrm{d}V\,\mathrm{d}\Lambda\Bigg\rangle. \end{aligned} \tag{2.16}$$

This is the generalisation of Seis's (2015) expression (4.10) which can be recovered by setting $\boldsymbol{a}=\hat{\boldsymbol{x}}$, taking $\mathcal{S}(\Lambda)$ as the horizontal plane $z=\Lambda$ over $[0, L_x]\times[0, L_y]$ and $\hat{\boldsymbol{n}}=\hat{\boldsymbol{z}}$. Notably, there are new integrated volume terms because the linear momentum directed along $\mathcal{C}(\lambda, y)$ is not conserved but these turn out to be subdominant in what follows. From here, the exercise is to bound the right-hand side of (2.16) in terms of the energy dissipation rate ε and then to optimise over $\ell \in [0, 1/2]$ to produce the best bound on Gr as in Seis (2015). Since our focus is on establishing the scaling exponent of how Gr scales with ε rather than the secondary issue of producing the best estimate for the numerical prefactor, we proceed by employing straightforward conservative estimates. This has the advantage of securing our key result quickly and relatively clearly but more careful estimates could lower the (numerical) bound on Gr but not, we contend, the scaling exponent. Firstly,

$$\begin{aligned} Gr \;\leqslant\; \frac{1}{A\ell(1-\ell)}\Bigg\{&\Bigg\langle\int_{1-\ell}^{1}\int_{\mathcal{S}(\Lambda)}|\boldsymbol{a}\cdot\boldsymbol{u}||\boldsymbol{u}\cdot\hat{\boldsymbol{n}}|\,\mathrm{d}S\,\mathrm{d}\Lambda\Bigg\rangle + \Bigg\langle\int_{1-\ell}^{1}\int_{\mathcal{S}(\Lambda)}|\boldsymbol{u}\cdot(\hat{\boldsymbol{n}}\cdot\boldsymbol{\nabla})\boldsymbol{a}|\,\mathrm{d}S\,\mathrm{d}\Lambda\Bigg\rangle \\ &+ \Bigg\langle\int_{1-\ell}^{1}\int_{\mathcal{S}(\Lambda)}|\boldsymbol{a}\cdot(\hat{\boldsymbol{n}}\cdot\boldsymbol{\nabla})\boldsymbol{u}|\,\mathrm{d}S\,\mathrm{d}\Lambda\Bigg\rangle + \Bigg\langle\int_{0}^{\ell}\int_{\mathcal{S}(\Lambda)}|\boldsymbol{a}\cdot\boldsymbol{u}||\boldsymbol{u}\cdot\hat{\boldsymbol{n}}|\,\mathrm{d}S\,\mathrm{d}\Lambda\Bigg\rangle^{(1)} \\ &+ \Bigg\langle\int_{0}^{\ell}\int_{\mathcal{S}(\Lambda)}|\boldsymbol{u}\cdot(\hat{\boldsymbol{n}}\cdot\boldsymbol{\nabla})\boldsymbol{a}|\,\mathrm{d}S\,\mathrm{d}\Lambda\Bigg\rangle^{(2)} + \Bigg\langle\int_{0}^{\ell}\int_{\mathcal{S}(\Lambda)}|\boldsymbol{a}\cdot(\hat{\boldsymbol{n}}\cdot\boldsymbol{\nabla})\boldsymbol{u}|\,\mathrm{d}S\,\mathrm{d}\Lambda\Bigg\rangle^{(3)} \\ &+ \Bigg\langle\int_{1-\ell}^{1}\iiint_{\mathcal{V}(\Lambda)}|\boldsymbol{u}\cdot(\boldsymbol{u}\cdot\boldsymbol{\nabla})\boldsymbol{a}|\,\mathrm{d}V\,\mathrm{d}\Lambda\Bigg\rangle + \Bigg\langle\int_{1-\ell}^{1}\iiint_{\mathcal{V}(\Lambda)}|\boldsymbol{u}\cdot\boldsymbol{\nabla}^2\boldsymbol{a}|\,\mathrm{d}V\,\mathrm{d}\Lambda\Bigg\rangle \\ &+ \Bigg\langle\int_{0}^{\ell}\iiint_{\mathcal{V}(\Lambda)}|\boldsymbol{u}\cdot(\boldsymbol{u}\cdot\boldsymbol{\nabla})\boldsymbol{a}|\,\mathrm{d}V\,\mathrm{d}\Lambda\Bigg\rangle^{(4)} + \Bigg\langle\int_{0}^{\ell}\iiint_{\mathcal{V}(\Lambda)}|\boldsymbol{u}\cdot\boldsymbol{\nabla}^2\boldsymbol{a}|\,\mathrm{d}V\,\mathrm{d}\Lambda\Bigg\rangle^{(5)}\Bigg\} \end{aligned} \tag{2.17}$$

(the superscripts in parentheses are just labels). Each of the integrals in (2.17) need to be bounded by a function of ε. We focus on integrals concentrated at the lower boundary and treat first the integral, I_1, labelled $^{(1)}$ in (2.17). Firstly converting the surface integral into one over $\mathcal{A}$

$$I_1 \leqslant \Bigg\langle\int_0^\ell\iint_{\mathcal{A}}|\boldsymbol{a}|\sqrt{1+F_x^2+F_y^2}|\boldsymbol{u}|^2\,\mathrm{d}x\,\mathrm{d}y\,\mathrm{d}\Lambda\Bigg\rangle. \tag{2.18}$$

Then using the fundamental theorem of calculus since $\boldsymbol{u}(x,y,f(x,y))=\boldsymbol{0}$ (i.e. on $\mathcal{S}(0)$) and Cauchy–Schwarz gives

$$\begin{aligned}
I_1 &\leqslant \left\langle \int_0^\ell \iint_{\mathcal{A}} |\boldsymbol{a}|\sqrt{1+F_x^2+F_y^2}\left|\int_{f(x,y)}^{z}\frac{\partial \boldsymbol{u}}{\partial \bar{z}}\,\mathrm{d}\bar{z}\right|^2 \mathrm{d}x\,\mathrm{d}y\,\mathrm{d}\Lambda \right\rangle \\
&\leqslant \left\langle \int_0^\ell \iint_{\mathcal{A}} |\boldsymbol{a}|\sqrt{1+F_x^2+F_y^2}\left(\int_{f(x,y)}^{z} 1^2\,\mathrm{d}\bar{z}\int_{f(x,y)}^{z}\left|\frac{\partial \boldsymbol{u}}{\partial \bar{z}}\right|^2\mathrm{d}\bar{z}\right)\mathrm{d}x\,\mathrm{d}y,\,\mathrm{d}\Lambda \right\rangle \\
&\leqslant \left\langle \int_0^\ell \iint_{\mathcal{A}} |\boldsymbol{a}|\sqrt{1+F_x^2+F_y^2}\,\Lambda F_\lambda \int_{f(x,y)}^{z}\left|\frac{\partial \boldsymbol{u}}{\partial \bar{z}}\right|^2\mathrm{d}\bar{z}\,\mathrm{d}x\,\mathrm{d}y\,\mathrm{d}\Lambda \right\rangle \\
&\leqslant \max_{x,y,\lambda\in\mathcal{V}(\ell)}\left\{|\boldsymbol{a}|F_\lambda\sqrt{1+F_x^2+F_y^2}\right\}\int_0^\ell \Lambda d\Lambda \left\langle \iiint |\nabla \boldsymbol{u}|^2\,\mathrm{d}V \right\rangle \\
&\leqslant \max_{x,y,\lambda\in\mathcal{V}(\ell)}\left\{\sqrt{1+F_x^2}\sqrt{1+F_x^2+F_y^2}\right\}\times\frac{1}{2}\ell^2 A\varepsilon. \qquad (2.19)
\end{aligned}$$

Integral I_4 (labelled $^{(4)}$ in (2.17)) is treated similarly albeit with an extra integration in Λ giving rise to ℓ^3 in the estimate:

$$\begin{aligned}
I_4 &\leqslant \left\langle \int_0^\ell \iiint_{\mathcal{V}(\Lambda)} |\nabla \boldsymbol{a}||\boldsymbol{u}|^2\,\mathrm{d}V\,\mathrm{d}\Lambda \right\rangle \leqslant \left\langle \int_0^\ell \int_0^\Lambda \iint_{\mathcal{A}} F_\lambda |\nabla \boldsymbol{a}||\boldsymbol{u}|^2\,\mathrm{d}x\,\mathrm{d}y\,\mathrm{d}\lambda\,\mathrm{d}\Lambda \right\rangle \\
&\leqslant \max_{x,y,\lambda\in\mathcal{V}(\ell)}\left\{F_\lambda^2|\nabla \boldsymbol{a}|\right\}\int_0^\ell\int_0^\Lambda \lambda\,\mathrm{d}\lambda\,\mathrm{d}\Lambda\left\langle \iiint |\nabla \boldsymbol{u}|^2\,\mathrm{d}V \right\rangle \\
&\leqslant \max_{x,y,\lambda\in\mathcal{V}(\ell)}\left\{F_\lambda^2|\nabla \boldsymbol{a}|\right\}\times\frac{1}{6}\ell^3 A\varepsilon. \qquad (2.20)
\end{aligned}$$

The remaining integrals, I_2, I_3 and I_5, are treated as follows:

$$\begin{aligned}
I_2 &\leqslant \left\langle \iint_{\mathcal{A}}\int_{f(x,y)}^{F(x,y,\ell)} \frac{|\hat{\boldsymbol{n}}\cdot\nabla \boldsymbol{a}|\sqrt{1+F_x^2+F_y^2}}{F_\lambda}|\boldsymbol{u}|\,\mathrm{d}z\,\mathrm{d}x\,\mathrm{d}y \right\rangle \\
&\leqslant \left[\iiint_{\mathcal{V}(\ell)}\frac{|\hat{\boldsymbol{n}}\cdot\nabla \boldsymbol{a}|^2(1+F_x^2+F_y^2)}{F_\lambda^2}\,\mathrm{d}V\right]^{1/2}\left[\left\langle \iiint_{\mathcal{V}(\ell)}|\boldsymbol{u}|^2\,\mathrm{d}V\right\rangle\right]^{1/2} \\
&\leqslant \left[\iiint_{\mathcal{V}(\ell)}\frac{|\hat{\boldsymbol{n}}\cdot\nabla \boldsymbol{a}|^2(1+F_x^2+F_y^2)}{F_\lambda^2}\,\mathrm{d}V\right]^{1/2}\times\left[\max_{(x,y)\in\mathcal{A}}F_\lambda^2\right]^{1/2}\times\sqrt{\frac{1}{2}\ell^2 A\varepsilon} \\
&\leqslant \left[\frac{1}{A}\iint_{\mathcal{A}}\max_{\Lambda\in[0,\ell]}\left\{|\hat{\boldsymbol{n}}\cdot\nabla \boldsymbol{a}|^2(1+F_x^2+F_y^2)\right\}\frac{\mathrm{d}x\,\mathrm{d}y}{F_\lambda}\right]^{1/2}\times\left[\max_{(x,y)\in\mathcal{A}}F_\lambda^2\right]^{1/2}\times A\sqrt{\frac{1}{2}\ell^3\varepsilon}, \qquad (2.21)
\end{aligned}$$

where $\hat{\boldsymbol{n}}=(-F_x\hat{\boldsymbol{x}}-F_y\hat{\boldsymbol{y}}+\hat{\boldsymbol{z}})/\sqrt{1+F_x^2+F_y^2}$ and the last two lines follow using the same type of estimates as in (2.19) and noting that $F_\lambda=g(x,y)-f(x,y)$ is independent

of λ and strictly positive. Respectively

$$\begin{aligned} I_3 &\leqslant \left\langle \iint_{\mathcal{A}} \int_{f(x,y)}^{F(x,y,\ell)} \frac{|\boldsymbol{a}|\sqrt{1+F_x^2+F_y^2}}{F_\lambda} |\nabla \boldsymbol{u}| \,\mathrm{d}z\,\mathrm{d}x\,\mathrm{d}y \right\rangle \\ &\leqslant \left[\iiint_{\mathcal{V}(\ell)} \frac{|\boldsymbol{a}|^2(1+F_x^2+F_y^2)}{F_\lambda^2} \,\mathrm{d}V \right]^{1/2} \times \sqrt{A\varepsilon} \\ &\leqslant \left[\iint_{\mathcal{A}} \int_0^\ell \frac{(1+F_x^2)(1+F_x^2+F_y^2)}{F_\lambda^3} \,\mathrm{d}\Lambda\,\mathrm{d}x\,\mathrm{d}y \right]^{1/2} \times \sqrt{A\varepsilon} \\ &\leqslant \left[\frac{1}{A} \iint_{\mathcal{A}} \max_{\Lambda\in[0,\ell]} \left\{ (1+F_x^2)(1+F_x^2+F_y^2) \right\} \frac{\mathrm{d}x\,\mathrm{d}y}{F_\lambda^3} \right]^{1/2} \times A\sqrt{\ell\varepsilon} \end{aligned} \tag{2.22}$$

and

$$\begin{aligned} I_5 &\leqslant \int_0^\ell \left[\iiint_{\mathcal{V}(\ell)} |\nabla^2 \boldsymbol{a}|^2 \,\mathrm{d}V \right]^{1/2} \left[\left\langle \iiint_{\mathcal{V}(\ell)} |\boldsymbol{u}|^2 \,\mathrm{d}V \right\rangle \right]^{1/2} \mathrm{d}\Lambda \\ &\leqslant \left[\frac{1}{A} \iiint_{\mathcal{V}(\ell)} |\nabla^2 \boldsymbol{a}|^2 \,\mathrm{d}V \right]^{1/2} \times \left[\max_{(x,y)\in\mathcal{A}} F_\lambda^2 \right]^{1/2} \times \ell^2 A \sqrt{\frac{1}{2}\varepsilon} \\ &\leqslant \left[\frac{1}{A} \iint_{\mathcal{A}} F_\lambda \max_{\Lambda\in[0,\ell]} |\nabla^2 \boldsymbol{a}|^2 \,\mathrm{d}x\,\mathrm{d}y \right]^{1/2} \times \left[\max_{(x,y)\in\mathcal{A}} F_\lambda^2 \right]^{1/2} \times A\sqrt{\frac{1}{2}\ell^5\varepsilon}. \end{aligned} \tag{2.23}$$

The estimates for the corresponding integrals centred at the top boundary are exactly analogous, and grouping the contributions together for each term, we get a simplified 'inequality' version of (2.16)

$$Gr \leqslant \frac{1}{\ell(1-\ell)} \{ (B_1\ell^2 + B_4\ell^3)\varepsilon + (B_2\ell + B_3 + B_5\ell^2)\sqrt{\ell\varepsilon} \}. \tag{2.24}$$

where the coefficients B_i represent the O(1) numerical factors (in the sense of $Gr \to \infty$) of the ith integral bound (summed for both boundaries) when a factor of A is factored out and the dominant ℓ and ε behaviour (which both are not $O(1)$) is separated off. The idea now is to minimise the right-hand side over the choice of $\ell \in (0,\, 1/2)$ in the turbulent limit $Gr \to \infty$. Here, $\varepsilon \to \infty$ (naive scalings suggest $Gr \lesssim \varepsilon \lesssim Gr^2$) and the optimal $\ell \to 0$ so, working to leading order,

$$Gr \leqslant B_1\ell\varepsilon + B_3\sqrt{\varepsilon/\ell} + \text{h.o.t.} \tag{2.25}$$

and now it is clear that all the new integral contributions due to the roughness are subdominant. Instead the roughness manifests itself as adjusted numerical coefficients for the integrals which arise in the smooth situation (Seis 2015). The minimising ℓ is $(B_3/2B_1)^{2/3}\varepsilon^{-1/3}$ and

$$Gr \leqslant \frac{3}{2}(2B_1B_3^2)^{1/3} \times \varepsilon^{2/3} \quad \text{or} \quad \frac{2\sqrt{3}}{9B_3\sqrt{B_1}} \times Gr^{3/2} \leqslant \varepsilon, \tag{2.26a,b}$$

where

$$B_1 = \sum_{\lambda=0}^{1} \max_{(x,y)\in\mathcal{A}} \left\{ \frac{1}{2}\sqrt{1+F_x^2}\sqrt{1+F_x^2+F_y^2} \right\}, \tag{2.27}$$

$$B_3 = \sum_{\lambda=0}^{1} \left[\frac{1}{A} \iint_{\mathcal{A}} \frac{(1+F_x^2)(1+F_x^2+F_y^2)}{[g(x,y)-f(x,y)]^3} \,\mathrm{d}x\,\mathrm{d}y \right]^{1/2} \tag{2.28}$$

(since $\ell \ll 1$, it is sufficient to leading order to replace $\max_{\Lambda\in[0,\ell]}$ by the value at $\Lambda = 0$ and similarly for the upper boundary). The lower bound in (2.26) indicates that turbulence decreases dissipation for a given applied pressure gradient as per the smooth wall case (Constantin & Doering 1995; Seis 2015). However, as there, rewriting the result in terms of the *a priori* unknown mean flow recovers the familiar upper bound situation. Taking $\langle \int\int\int \boldsymbol{u} \cdot (2.1)\,\mathrm{d}V \rangle$ connects the mean flow U with the applied pressure gradient and ensuing dissipation rate,

$$U := \left\langle \frac{1}{A} \iiint \boldsymbol{u}\cdot\hat{\boldsymbol{x}}\,\mathrm{d}V \right\rangle = \varepsilon/Gr. \tag{2.29}$$

This can be used to eliminate the pressure gradient (Gr) to get

$$\varepsilon \leqslant \tfrac{27}{4} B_1 B_3^2 U^3 \quad \text{or} \quad \varepsilon \leqslant \tfrac{27}{4} B_1 B_3^2 \quad (\text{in units of } U^3/h) \tag{2.30a,b}$$

so that the bound predicts that the energy dissipation rate becomes independent of the viscosity as the viscosity goes to zero – Kolmogorov scaling – just as in the smooth wall calculation (Constantin & Doering 1995; Seis 2015, and Plasting & Kerswell 2005 for pipe flow).

3. Oscillatory flow across topography: the tidal problem

As a simple application of the above result, we now consider the ocean tidal problem of oscillatory flow across bottom topography (and a free top surface). This situation is modelled by assuming an oscillatory pressure gradient driving the flow directly i.e. $\mathcal{G} \sim \omega^* U^*$ where the tidal frequency $\omega^* = 2\pi/12$ hours $= 1.4 \times 10^{-4}$ s^{-1} and $U^* \approx 0.1$ m s^{-1}. We consider a symmetrised problem where the top boundary is defined by $g(x, y) = 1 - f(x, y)$ so that the real free surface position on average is the (symmetric) midplane of the extended domain and $h/2$ is then the mean ocean depth. By symmetry, the maximum dissipation in the extended domain is exactly double the maximum dissipation in the 'ocean' domain. Further restricting the flow in the extended domain to have zero vertical motion and zero stress across $z = 1/2$ (the horizontal free-surface approximation) can only reduce the maximum dissipation possible (by restricting the competitor space) so halving the dissipation bound from the unrestricted, extended domain should be an upper bound on the dissipation in a flat surface ocean ($z \leqslant 1/2$).

Taking a typical ocean depth $h/2 = 1000$ m, the Grashof number $Gr = 1.12 \times 10^{17} \gg 1$ and the non-dimensionalised tidal frequency

$$1 \ll \omega := \frac{h^2\omega^*}{\nu} = \sqrt{\frac{h\mathcal{G}}{U^2}}\sqrt{Gr} \ll Gr, \tag{3.1}$$

where $\Upsilon := h\mathcal{G}/U^2$ is a second non-dimensional number independent of ν which is here $O(1)$. This makes it clear that in the limit $\nu \to 0$ (with everything else kept fixed), $Gr \to \infty$ with $\omega \sim \sqrt{Gr}$. The governing equation for the problem is then

$$\frac{\partial \boldsymbol{u}}{\partial t} + 2\boldsymbol{\Omega} \times \boldsymbol{u} + \boldsymbol{u}\cdot\nabla\boldsymbol{u} + \nabla p - \nabla^2\boldsymbol{u} = Gr\, \Gamma(t)\hat{\boldsymbol{x}}, \tag{3.2}$$

the flow is assumed incompressible and a planetary rotation $\boldsymbol{\Omega}$ is also included for completeness ($|\boldsymbol{\Omega}| = \omega/2$). The oscillatory function $\Gamma(t)$ is defined such that

$$\max_{t\in[0,2\pi/\omega]} |\Gamma(t)| = 1 \tag{3.3}$$

but is otherwise left unspecified for clarity. As before, the analysis starts by taking the line integral of (3.2) along $\mathcal{C}(\lambda, y)$ and integrating over y as above in § 2 but now also multiplying by $\Gamma(t)$ to rectify the forcing pressure gradient. This leads to an extended version of (2.8)

$$\begin{aligned} AGr\Gamma(t)^2 \;=\; & \Gamma(t)\frac{\partial}{\partial t}\iint_{\mathcal{A}} (\hat{\boldsymbol{x}} + F_x\hat{\boldsymbol{z}})\cdot\boldsymbol{u}\,\mathrm{d}x\,\mathrm{d}y \\ & + \Gamma(t)\iint_{\mathcal{A}} (\hat{\boldsymbol{x}} + F_x\hat{\boldsymbol{z}})\cdot[2\boldsymbol{\Omega}\times\boldsymbol{u} + \boldsymbol{u}\cdot\boldsymbol{\nabla}\boldsymbol{u} - \nabla^2\boldsymbol{u}]\,\mathrm{d}x\,\mathrm{d}y. \end{aligned} \tag{3.4}$$

Now long-time averaging leads to

$$\begin{aligned} AGr\langle\Gamma(t)^2\rangle \;=\; & -\left\langle \Gamma_t \iint_{\mathcal{A}} (\hat{\boldsymbol{x}} + F_x\hat{\boldsymbol{z}})\cdot\boldsymbol{u}\,\mathrm{d}x\,\mathrm{d}y\right\rangle \\ & + \left\langle \Gamma(t)\iint_{\mathcal{A}} (\hat{\boldsymbol{x}} + F_x\hat{\boldsymbol{z}})\cdot[2\boldsymbol{\Omega}\times\boldsymbol{u} + \boldsymbol{u}\cdot\boldsymbol{\nabla}\boldsymbol{u} - \nabla^2\boldsymbol{u}]\,\mathrm{d}x\,\mathrm{d}y\right\rangle, \end{aligned} \tag{3.5}$$

where integration by parts in time has been used to transfer the time derivative onto Γ. Integrating over $\lambda\in[0,\Lambda]$ and converting to a volume integral over $\mathcal{V}(\Lambda)$, gives

$$\Lambda Gr\langle\Gamma(t)^2\rangle = \frac{1}{A}\left\langle \iiint_{\mathcal{V}(\Lambda)} \Gamma(t)\boldsymbol{a}\cdot[\boldsymbol{u}\cdot\boldsymbol{\nabla}\boldsymbol{u} - \nabla^2\boldsymbol{u}] + [\Gamma\boldsymbol{a}\times 2\boldsymbol{\Omega} - \Gamma_t\boldsymbol{a}]\cdot\boldsymbol{u}\,\mathrm{d}x\,\mathrm{d}y\,\mathrm{d}z\right\rangle \tag{3.6}$$

for all $\Lambda\in[0,1]$. The first term on the right-hand side is as before, albeit with an extra factor of $\Gamma(t)$. Since this is bounded in modulus by 1, the subsequent estimates are unchanged. The new second term on the right-hand side is of the form of I_5 and can be similarly estimated as adding a new term

$$\left[\frac{1}{A}\iint_{\mathcal{A}} F_\lambda \max_{\Lambda\in[0,\ell]} |\Gamma\boldsymbol{a}\times 2\boldsymbol{\Omega} - \Gamma_t\boldsymbol{a}|^2\,\mathrm{d}x\,\mathrm{d}y\right]^{1/2} \times \left[\max_{(x,y)\in\mathcal{A}} F_\lambda^2\right]^{1/2} \times A\sqrt{\frac{1}{2}\ell^5\varepsilon} \tag{3.7}$$

to (2.24). Since both $\boldsymbol{\Omega}$ and $\Gamma_t = O(\omega\Gamma)$ are $O(\sqrt{Gr})$, the leading-order version of (2.24) is potentially modified to

$$Gr \leqslant B_1\ell\varepsilon + (B_3 + B_5\ell^2\sqrt{Gr})\sqrt{\varepsilon/\ell} + \text{h.o.t.} \tag{3.8}$$

The minimiser, however, remains $\ell\sim\varepsilon^{-1/3}$ with the new term $O(Gr^{-1/2})$ smaller than the other two terms. Hence the rotation and oscillation are not important at leading order in the bound on the energy dissipation rate for tidal flow over topography.

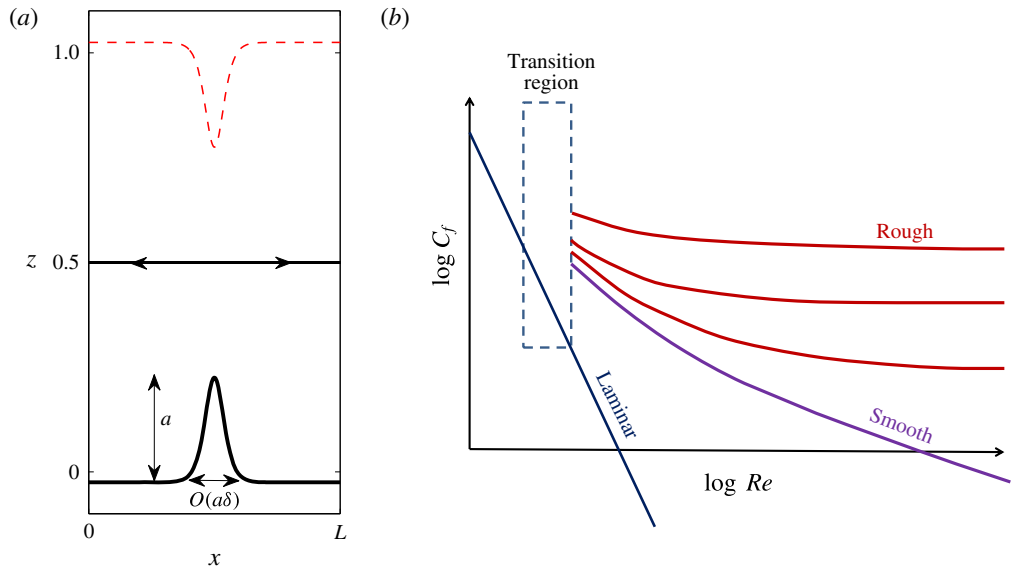

FIGURE 2. (Colour online) (*a*) The 2-D ridge tidal problem with the ocean represented by the region $z \leqslant 1/2$. (*b*) A cartoon of the Moody diagram for pipe flow (Moody 1944): $C_f := \varepsilon/(U^3/h)$, laminar flow has $C_f \sim 1/Re$, turbulent smooth pipe data suggest $C_f \sim 1/(\log Re)^2$ at least to $Re = O(10^8)$ and turbulent rough pipe data have $C_f \sim O(1)$ as $Re \to \infty$. Three lines are shown for rough pipe flow with the data increasing to higher C_f as the representative height of the roughness increases.

3.1. *A simple example*

Here we consider a 2-D ridge of height $a < 1/2$ and horizontal extent $a\delta$

$$f(x) := a\,\mathrm{sech}^2\left(\frac{x - \frac{1}{2}L}{a\delta}\right) - \frac{2a^2\delta}{L}\tanh\left(\frac{L}{2a\delta}\right) \tag{3.9}$$

over $x \in [0, L]$ (the second term on the right-hand side ensures the roughness has zero mean over x): see figure 2. This roughness function is not periodic over $[0, L]$ but in the steep ($\delta \ll 1$) isolated ($a\delta \ll L$) ridge limit this can be ignored. In this limit, it is straightforward to approximate B_1 and B_3 as follows

$$B_1 = \max_{x\in[0,L]}(1 + f_x^2) \approx \frac{16}{27\delta^2}, \quad B_3 = 2\left[\frac{1}{L}\int \frac{(1+f_x^2)^2}{(1-2f)^3}\,\mathrm{d}x\right]^{1/2} \lesssim \left[\frac{2a}{L(1-2a)^3\delta^3}\right]^{1/2}, \tag{3.10}$$

(using the fact that $2048/1155 < 2$) so the dissipation rate per unit mass is

$$\varepsilon \leqslant \frac{4aU^3}{L(1-2a)^3\delta^5} \quad \text{(in units of } \nu^3/h^4\text{)} \tag{3.11}$$

(including the $1/2$ to reflect the fact that the ocean is strictly in $z \leqslant 1/2$). This can be re-expressed using inertial units to give the familiar bound independent of the viscosity

$$\varepsilon \leqslant \frac{4a}{L(1-2a)^3\delta^5} \quad \text{(in units of } U^3/h\text{)}. \tag{3.12}$$

Since this is the leading term due to the ridge (the dissipation bound for zero topography is $O(\delta^5)$ smaller), this expression can be viewed as giving the enhanced dissipation caused by the ridge per unit length of the domain $[0, L]$.

4. Discussion

Using a new bounding technique (Otto & Seis 2011; Seis 2015), this paper has derived an upper bound on the energy dissipation rate (per unit mass) ε for pressure-driven flow through a rough channel with bottom $z = f(x, y)$ and top $z = g(x, y)$ (f and g at least C^3) such that the average height is h in the limit of vanishing viscosity of the form

$$\varepsilon \leqslant cU^3/h, \tag{4.1}$$

where U is the mean flow through the channel and

$$c := \frac{27}{8}\sum_{\lambda=0}^{1}\max_{(x,y)\in\mathcal{A}}\left\{\sqrt{1+F_x^2}\sqrt{1+F_x^2+F_y^2}\right\} \times\left(\sum_{\lambda=0}^{1}\left[\frac{1}{A}\iint_{\mathcal{A}}\frac{(1+F_x^2)(1+F_x^2+F_y^2)}{[g(x,y)-f(x,y)]^3}\,\mathrm{d}x\,\mathrm{d}y\right]^{1/2}\right)^2, \tag{4.2}$$

with $F(x, y, \lambda) := (1-\lambda)f(x, y) + \lambda g(x, y)$ and $\mathcal{A} := [0, L_x] \times [0, L_y]$. The fact that bound predicts that the dissipation rate approaches a finite limit (in inertial units) as the viscosity vanishes – so-called Kolmogorov scaling – then captures the observed scaling of turbulent data in rough pipes – see figure 2 for a cartoon of the classic Moody diagram (Moody 1944) – and indicates that the well-known discrepancy between the bound and data scalings in the smooth wall case (Constantin & Doering (1995), Plasting & Kerswell (2005), Seis (2015) and figure 2) is an exception rather than the rule. Interestingly, boundary cross-flow produced by suction instead of roughness also seems to achieve the same effect in plane Couette flow: bounds and data have the same Kolmogorov scaling for non-zero suction but disagree for zero suction (Doering, Spiegel & Worthing 2000). These observations, which may also extend to convection although the available data are so far only suggestive (see Goluskin & Doering 2016), substantially enhance the credentials of the bounding approach as a viable way to extract key scaling laws in real turbulent flows where smooth walls are not generic.

There is, of course, room for improvement. The bound derived here requires C^3 differentiability of the roughness whereas it would be better (and more realistic) to only require continuity and piecewise differentiability. This would allow sharp corners, such as those present in roughness created by sand granules, to be treated. It is possible that better functional analytic estimates may achieve this as well as reducing the numerical prefactor c (e.g. by replacing the infinity norm present by a less extreme norm). However, it seems difficult to see how the exponent in the scaling law (i.e. $\varepsilon \sim Re^0U^3/h$ as $Re \to \infty$) could be changed. From a mathematical perspective, formulating the full variational equations underlying the Otto–Seis 'boundary layer' method presents an enticing challenge with the potential for revealing valuable insights into this new method. It was, after all, only after the full variational equations were identified for the Doering–Constantin background method that an intimate connection was made to the Malkus–Howard–Busse bounding approach (Kerswell 1997, 1998).

A significant challenge for the bounding approach remains, however, deriving a dissipation bound on shearing systems with rough boundaries (e.g. rough plane

Couette flow). Here, unlike pressure-driven flow through a stationary rough channel, one rough boundary moving relative to another means that there has to be motion locally perpendicular to one boundary and therefore work done by the pressure enters the calculation. So far all bounding approaches eliminate the pressure as soon as possible so a totally different approach will be needed. Nevertheless it is reasonable to suppose that a dissipation bound will be derived with Kolmogorov scaling which is what is observed in rough-walled Taylor–Couette flow. If one or both of the walls are smooth, however, the observed dissipation rate then drops off like $\sim 1/(\log Re)^2$ mimicking the situation in pipe flow (Cadot *et al.* 1997; van den Berg *et al.* 2003).

Finally, an application of the new bound has been made to a problem of interest in ocean modelling. This warrants further development to include stable stratification and a refocus on the turbulent mixing that can be caused by isolated topography (typically by internal wave breaking) as this is an important yet poorly known input in ocean models (e.g. see Melet *et al.* (2016) and references therein).

Acknowledgement

Many thanks to the referees who helped eliminate some typos in the submitted manuscript.

REFERENCES

VAN DEN BERG, T. H., DOERING, C. R., LOHSE, D. & LATHROP, D. P. 2003 Smooth and rough boundaries in turbulent Taylor–Couette flow. *Phys. Rev.* E **68**, 036307.

BUSSE, F. H. 1969 Bounds on the transport of mass and momentum by turbulent flow between parallel plates. *Z. Angew. Math. Phys.* **20**, 1–14.

BUSSE, F. H. 1970 Bounds for turbulent shear flows. *J. Fluid Mech.* **41**, 219–240.

BUSSE, F. H. 1978 The optimal theory of turbulence. *Adv. Appl. Mech.* **18**, 77–121.

CADOT, O., COUDER, Y., DAERR, A., DOUADY, S. & TSINOBER, A. 1997 Energy injection in closed turbulent flows: stirring through boundary layers versus inertial stirring. *Phys. Rev.* E **56**, 427–433.

CONSTANTIN, P. & DOERING, C. R. 1995 Variational bounds on energy dissipation in incompressible flows. II: channel flow. *Phys. Rev.* E **51**, 3192–3198.

DOERING, C. R. & CONSTANTIN, P. 1992 Energy dissipation in shear driven turbulence. *Phys. Rev. Lett.* **69**, 1648–1651.

DOERING, C. R. & CONSTANTIN, P. 1994 Variational bounds on energy dissipation in incompressible flows. shear flow. *Phys. Rev.* E **49**, 4087–4099.

DOERING, C. R. & CONSTANTIN, P. 1996 Variational bounds on energy dissipation in incompressible flows. III: convection. *Phys. Rev.* E **53**, 5957–5981.

DOERING, C. R., SPIEGEL, E. A. & WORTHING, R. A. 2000 Energy dissipation in a shear layer with suction. *Phys. Fluids* **12**, 1955–1968.

DOERING, C. R. & CONSTANTIN, P. 2001 On upper bounds for infinite Prandtl number convection with and without rotation. *J. Math. Phys.* **42**, 784–795.

DOERING, C. R. & FOIAS, C. 2002 Energy dissipation in body-forced turbulence. *J. Fluid Mech.* **467**, 289–306.

FRISCH, U. 1995 *Turbulence*. Cambridge University Press.

GOLUSKIN, D. & DOERING, C. R. 2016 Bounds for convection between rough boundaries. *J. Fluid Mech.* **804**, 370–386.

GROSSMANN, S. & LOHSE, D. 2000 Scaling in thermal convection: a unifying theory. *J. Fluid Mech.* **407**, 27–56.

HOFFMANN, N. P. & VITANOV, N. K. 1999 Upper bounds on energy dissipation in Couette–Ekman flow. *Phys. Lett.* A **255**, 277–286.

HOWARD, L. N. 1963 Heat transport by turbulent convection. *J. Fluid Mech.* **17**, 405–432.

HOWARD, L. N. 1972 Bounds on flow quantities. *Annu. Rev. Fluid Mech.* **4**, 473–494.

KERSWELL, R. R. 1996 Upper bounds on the energy dissipation in turbulent precession. *J. Fluid Mech.* **321**, 335–370.

KERSWELL, R. R. 1997 Variational bounds on shear-driven turbulence and turbulent Boussinesq convection. *Physica* D **100**, 355–376.

KERSWELL, R. R. 1998 Unification of variational principles for turbulent shear flows: the background method of Doering–Constantin and the mean-fluctuation formulation of Howard–Busse. *Physica* D **101**, 178–190.

KERSWELL, R. R. 2002 Upper bounds on general dissipation functionals in turbulent shear flows: revisiting the 'efficiency' functional. *J. Fluid Mech.* **461**, 239–275.

MALKUS, W. V. R. 1954 The heat transport and spectrum of thermal turbulence. *Proc. R. Soc. Lond.* A **225**, 196–212.

MARCHIORO, C. 1994 Remark on the energy dissipation in shear driven turbulence. *Physica* D **74**, 395–398.

MELET, A., LEGG, S. & HALLBERG, R. 2016 Climate impacts of parameterized local and remote tidal mixing. *J. Clim.* **29**, 3473–3500.

MOODY, L. F. 1944 Friction factors for pipe flow. *Trans. ASME* **66**, 671–684.

NICODEMUS, R., GROSSMANN, S. & HOLTHAUS, M. 1997 Improved variational principle for bounds on energy dissipation in turbulent shear flow. *Physica* D **101**, 178–190.

NOBILI, C. & OTTO, F. 2016 Limitations of the background field method applied to Rayleigh–Bénard convection. *J. Math. Phys.* (in press). arXiv:1605:08135.

OTERO, J., WITTENBERG, R. W., WORTHING, R. A. & DOERING, C. R. 2002 Bounds on Rayleigh–Bénard convection with an imposed heat flux. *J. Fluid Mech.* **473**, 191–199.

OTTO, F. & SEIS, C. 2011 Rayleigh–Bénard convection: improved bounds on the Nusselt number. *J. Math. Phys.* **52**, 083702,1–24.

PLASTING, S. C. & KERSWELL, R. R. 2003 Improved upper bound on the energy dissipation rate in plane Couette flow: the full solution to Busse's problem and the Constantin–Doering–Hopf problem with one-dimensional background field. *J. Fluid Mech.* **477**, 363–379.

PLASTING, S. C. & KERSWELL, R. R. 2005 A friction factor bound for transitional pipe flow. *Phys. Fluids* **17**, 011706.

PLASTING, S. C. & IERLEY, G. R. 2005 Infinite-Prandtl number convection. Part 1. Conservative bounds. *J. Fluid Mech.* **542**, 343–363.

SEIS, C. 2015 Scaling bounds on dissipation in turbulent flows. *J. Fluid Mech.* **777**, 591–603.

WALEFFE, F., BOONKASAME, A. & SMITH, L. M. 2015 Heat transport by coherent Rayleigh–Bénard convection. *Phys. Fluids* **27**, 051702.

WEN, B., CHINI, G. P., DIANATI, N. & DOERING, C. R. 2013 Computational approaches to aspect-ratio-dependent upper bounds and heat flux in porous medium convection. *Phys. Lett.* A **377**, 2931–2938.

WANG, X. 1997 Time averaged energy dissipation rate for shear driven flows in $\mathbb{R}^n$. *Physica* D **99**, 555–563.

WHITEHEAD, J. P. & DOERING, C. R. 2011 Ultimate state of two-dimensional Rayleigh–Bénard convection between free-slip fixed temperature boundaries. *Phys. Rev. Lett.* **106**, 244501.

WHITEHEAD, J. P. & WITTENBERG, R. W. 2014 A rigorous bound on the vertical transport of heat in Rayleigh–Bénard convection at infinite Prandtl number with mixed thermal boundary conditions. *J. Math. Phys.* **55**, 093104.

WITTENBERG, R. W. 2010 Bounds on Rayleigh–Bénard convection with imperfectly conducting plates. *J. Fluid Mech.* **665**, 158–198.